AGT

Algebraic & Geometric Topology

Volume 24 (2024)

Combinatorial proof of Maslov index formula in Heegaard Floer theory

Roman Krutowski

msp

Algebraic & Geometric Topology **24**:8 (2024) 4471–4485
DOI: 10.2140/agt.2024.24.4471
Published: 17 December 2024

Combinatorial proof of Maslov index formula in Heegaard Floer theory

ROMAN KRUTOWSKI

We prove Lipshitz's Maslov index formula in Heegaard Floer homology via the combinatorics of Heegaard diagrams.

57K18; 57K31

1 Introduction

Peter Ozsváth and Zoltán Szabó [2004b; 2004c] introduced Heegaard Floer homology, a collection of invariants for closed oriented 3–manifolds. Since then, Heegaard Floer homology has emerged as an extremely powerful invariant, producing strong results in low-dimensional topology (see [Ghiggini 2008; Ni 2009a; 2009b; Ozsváth and Szabó 2004a; 2004b; 2004c; 2006]). All of the numerous versions of Heegaard Floer homology involve counting the number of points in the unparametrized moduli space of J–holomorphic disks of a certain Maslov index joining some intersection points of two half-dimensional tori in a certain symmetric product of a surface.

The most notable advantage of Heegaard Floer homology when compared to other types of Floer homology is its combinatorial nature which allows computation of these invariants in various cases. One of the ingredients is the combinatorial formula for the Maslov index $\mu(\varphi)$ of a Whitney disk φ, which is the Fredholm index of some differential operator, or alternatively, a homology class of a certain loop in the Lagrangian Grassmannian. Jacob Rasmussen [2003] gave a formula that relates the intersection number of the disk with the fat diagonal in the symmetric product, with its Maslov index. Later on, Robert Lipshitz [2006], in a paper devoted to the cylindrical reformulation of the whole theory, gave a purely combinatorial formula for the Maslov index of these disks.

The proof of this formula in [Lipshitz 2006] is based on an elegant geometric approach. In this paper, we provide a combinatorial proof of this formula which is inspired by the proof of the index formula for Maslov n–gons due to Sucharit Sarkar [2011].

Let $(\Sigma, \boldsymbol{\alpha}, \boldsymbol{\beta})$ be a Heegaard diagram. Any Whitney disk $\varphi \in \pi_2(\boldsymbol{x}, \boldsymbol{y})$ connecting $\boldsymbol{x}, \boldsymbol{y} \in \mathrm{Sym}^g(\Sigma)$ has a *shadow* $D(\varphi)$ (see Definition 2.1), a certain 2–chain in Σ with boundary satisfying $\partial(\partial D(\varphi) \cap \boldsymbol{\alpha}) = \boldsymbol{y} - \boldsymbol{x}$ and $\partial(\partial D(\varphi) \cap \boldsymbol{\beta}) = \boldsymbol{x} - \boldsymbol{y}$. We denote the set of such 2–chains by $\mathfrak{D}(\boldsymbol{x}, \boldsymbol{y})$ and call them *domains*. We denote by $\mathfrak{D}$ the set of all domains in all Heegaard diagrams (see Section 2 for details).

In this paper, we assume that $\boldsymbol{\alpha}$ curves intersect $\boldsymbol{\beta}$ curves perpendicularly with respect to some metric on Σ. Among the domains, there are two special types that serve us as building blocks. *Bigons* and *rectangles* are 2–sided and 4–sided domains, respectively, which are homeomorphic to disks with all angles equal to 90° and which do not contain any $\boldsymbol{x}$– and $\boldsymbol{y}$–coordinates in the interior.

Given two domains $D \in \mathfrak{D}(\boldsymbol{x}, \boldsymbol{y})$ and $D' \in \mathfrak{D}(\boldsymbol{y}, \boldsymbol{z})$ the composition of these domains $D * D'$ is a domain $D + D' \in \mathfrak{D}(\boldsymbol{x}, \boldsymbol{z})$.

In this paper any map $\overline{\mu}\colon \mathfrak{D} \to \mathbb{Z}$ will be called an *index*. An index $\overline{\mu}$ is said to be *additive* if for any Heegaard diagram and any two of its domains $D \in \mathfrak{D}(\boldsymbol{x}, \boldsymbol{y})$ and $D' \in \mathfrak{D}(\boldsymbol{y}, \boldsymbol{z})$,

$$\overline{\mu}(D * D') = \overline{\mu}(D) + \overline{\mu}(D').$$

In Section 2 we introduce two types of transformations of any Heegaard diagram $(\Sigma, \boldsymbol{\alpha}, \boldsymbol{\beta})$ which assign to each of its domain D a new domain D' in the new Heegaard diagram. These transformations are called *finger moves* and *empty stabilizations*. An index $\overline{\mu}$ is said to be *stable* if for any such transformation $\overline{\mu}(D) = \overline{\mu}(D')$.

Define the *combinatorial index* $\widetilde{\mu}$ of a domain $D \in \mathfrak{D}(\boldsymbol{x}, \boldsymbol{y})$ via the formula due to Lipshitz [2006],

$$\widetilde{\mu}(D) := \widetilde{\mu}_{\boldsymbol{x}}(D) + \widetilde{\mu}_{\boldsymbol{y}}(D) + e(D), \tag{1}$$

where $\widetilde{\mu}_{\boldsymbol{x}}(D)$ is a point measure of D at $\boldsymbol{x}$ and $e(D)$ is the Euler measure of D (see Section 2.1).

We are now ready to formulate our main results.

Theorem 1.1 *There exists a unique index $\overline{\mu}\colon \mathfrak{D} \to \mathbb{Z}$ satisfying the following axioms*:

(1) *$\overline{\mu}$ is additive*;
(2) *$\overline{\mu}$ is stable*;
(3) *$\overline{\mu}(B) = 1$ for any bigon $B \in \mathfrak{D}$*;
(4) *$\overline{\mu}(R) = 1$ for any rectangle $R \in \mathfrak{D}$.*

Moreover, this index agrees with the combinatorial index $\widetilde{\mu}$.

Theorem 1.2 *Let $(\Sigma, \boldsymbol{\alpha}, \boldsymbol{\beta})$ be a Heegaard diagram and φ be a Whitney disk connecting two generators of the corresponding Heegaard Floer chain complex. Then*

$$\mu(\varphi) = \widetilde{\mu}(D(\varphi)),$$

where $\mu(\varphi)$ is the Maslov index of φ.

Acknowledgements I would like to thank Sucharit Sarkar for his guidance and encouragement, Ko Honda for helpful conversations and suggestions, and Gleb Terentiuk for valuable comments. I thank Vinicius Canto Costa for pointing out some minor errors in a previous version. I thank the referee for numerous helpful comments and corrections.

2 Notations and preliminary results

2.1 Heegaard Floer theory preliminaries

To start, recall the definition of a Heegaard diagram. Let Σ be an oriented closed Riemannian surface (ie there is a fixed Riemannian metric) and $\boldsymbol{\alpha} = \{\alpha_1, \dots, \alpha_g\}$ and $\boldsymbol{\beta} = \{\beta_1, \dots, \beta_g\}$ be two sets of nonintersecting *oriented*[1] simple closed curves such that both $\boldsymbol{\alpha}$ and $\boldsymbol{\beta}$ generate half-dimensional subspaces of $H_1(\Sigma)$ (in particular this means that g is not smaller than the genus $g(\Sigma)$ of the surface). The last part is equivalent to assuming that the complement of $\boldsymbol{\alpha}$ consists of $g - g(\Sigma) + 1$ components (the same holds for $\boldsymbol{\beta}$). We also assume that the $\boldsymbol{\alpha}$ and $\boldsymbol{\beta}$ curves intersect perpendicularly. We call by *regions* closures of connected components of $\Sigma \setminus (\boldsymbol{\alpha} \cup \boldsymbol{\beta})$. The collection $(\Sigma, \boldsymbol{\alpha}, \boldsymbol{\beta})$ is usually called an *unpointed Heegaard diagram*, but in the text we refer to it simply as a *Heegaard diagram*. We need not assume these diagrams to be pointed, because it is not relevant for the Maslov index calculations.

The Heegaard Floer homology chain complex of a diagram $(\Sigma, \boldsymbol{\alpha}, \boldsymbol{\beta})$ is generated by g–tuples of points of the form $\boldsymbol{x} = \{x_1, \dots, x_g\}$ where $x_i \in \alpha_i \cap \beta_{\sigma(i)}$ and $\sigma \in S_g$ is arbitrary. We may regard $\boldsymbol{x}$ as a point in $\mathrm{Sym}^g(\Sigma)$ which belongs to $T_{\boldsymbol{\alpha}} \cap T_{\boldsymbol{\beta}}$ where $T_{\boldsymbol{\alpha}} = \alpha_1 \times \alpha_2 \times \cdots \times \alpha_g$ and $T_{\boldsymbol{\beta}} = \beta_1 \times \beta_2 \times \cdots \times \beta_g$.

Let us consider the unit disk D^2 in $\mathbb{C}$ with the usual orientation. Let $s_1 \subset \partial D^2$ be the portion of the oriented boundary that connects i to $-i$ and let $s_2 \subset \partial D^2$ be the remaining portion of the boundary connecting $-i$ to i. The differentials and chain maps are signed counts of J–holomorphic maps

$$u \colon D^2 \setminus \{i, -i\} \to \mathrm{Sym}^g(\Sigma)$$

representing Whitney disks in $\pi_2(\boldsymbol{x}, \boldsymbol{y})$. Here a Whitney disk is a homotopy type of maps from D^2 to $\mathrm{Sym}^g(\Sigma)$ such that s_1 is mapped to $T_{\boldsymbol{\alpha}}$, s_2 is mapped to $T_{\boldsymbol{\beta}}$, and i and $-i$ are sent to $\boldsymbol{x}$ and $\boldsymbol{y}$, respectively.

Let D be a 2–chain obtained as a sum of regions of a Heegaard diagram $(\Sigma, \boldsymbol{\alpha}, \boldsymbol{\beta})$ with integer coefficients, $D = \sum_R a(R) R$ where $a(R) \in \mathbb{Z}$. Such a 2–chain D is called a *domain* if there exist two generators $\boldsymbol{x}$ and $\boldsymbol{y}$ such that $\partial(\partial D|_{\boldsymbol{\alpha}}) := \partial(\partial D \cap \boldsymbol{\alpha}) = \boldsymbol{y} - \boldsymbol{x}$ (here we regard $\boldsymbol{x}$ and $\boldsymbol{y}$ as 0–chains in Σ) and $\partial(\partial D|_{\boldsymbol{\beta}}) = \boldsymbol{x} - \boldsymbol{y}$. We say that D *connects* $\boldsymbol{x}$ and $\boldsymbol{y}$ and denote the set of these domains by $\mathfrak{D}(\boldsymbol{x}, \boldsymbol{y})$. We also denote by $\mathfrak{D}$ the set of all pairs of $((\Sigma, \boldsymbol{\alpha}, \boldsymbol{\beta}), D)$, where the first element in the pair is some Heegaard diagram and the second is some domain in this Heegaard diagram.

Definition 2.1 Given a Whitney disk $\varphi \in \pi_2(\boldsymbol{x}, \boldsymbol{y})$ we associate a domain $D(\varphi) \in \mathfrak{D}(\boldsymbol{x}, \boldsymbol{y})$ called the *shadow* of φ as follows: to a region R we assign the number $n_R(\varphi)$ which is equal to the intersection number $\varphi \cdot Z_r$, where $Z_r = \{r\} \times \mathrm{Sym}^{g-1}(\Sigma)$ for some r in the interior of R (note that $\varphi \cdot Z_r$ does not depend on a choice of r); then set

$$D(\varphi) = \sum_R n_R(\varphi) R \in \mathfrak{D}(\boldsymbol{x}, \boldsymbol{y}).$$

[1]This is nonstandard but useful to assume for the entirety of the paper.

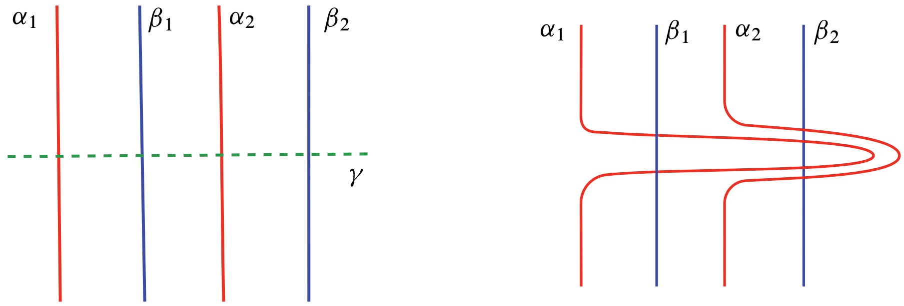

Figure 1: Finger move.

Let us recall the definition of the Maslov index of a Whitney disk $\varphi \in \pi_2(\boldsymbol{x}, \boldsymbol{y})$ where $\boldsymbol{x}$ and $\boldsymbol{y}$ are some generators of the chain complex associated with a given Heegaard diagram $(\Sigma, \boldsymbol{\alpha}, \boldsymbol{\beta})$. The generators $\boldsymbol{x}$ and $\boldsymbol{y}$ are regarded as points belonging to $T_{\boldsymbol{\alpha}} \cap T_{\boldsymbol{\beta}} \subset \mathrm{Sym}^g(\Sigma)$. Let Gr_g be a space of totally real g–dimensional subspaces of $\mathbb{C}^g$. Since φ is regarded as a map from $D^2 \setminus \{i, -i\} = [0,1] \times \mathbb{R}$ to $\mathrm{Sym}^g(\Sigma)$ we take the pullback of $T\,\mathrm{Sym}^g(\Sigma)$ to D^2 which is a trivial bundle $\underline{\mathbb{C}}^g$. One may then identify pullbacks of $T_{\boldsymbol{x}}(T_{\boldsymbol{\alpha}})$ and $T_{\boldsymbol{x}}(T_{\boldsymbol{\beta}})$ with two points $V_{\boldsymbol{x},\boldsymbol{\alpha}}, V_{\boldsymbol{x},\boldsymbol{\beta}} \in \mathrm{Gr}_g$. We pick a "short" path $\gamma_{\boldsymbol{x}}$ between $V_{\boldsymbol{x},\boldsymbol{\alpha}}$ and $V_{\boldsymbol{x},\boldsymbol{\beta}}$ in Gr_g and also construct in the same fashion a path $\gamma_{\boldsymbol{y}}$ for y (by "short" we mean a path in $\mathcal{P}^-(\mathrm{Gr}_g)$ in Seidel's terminology [2008, Section 11]). The map from $0 \times \mathbb{R}$ to $T_{\boldsymbol{\alpha}}$ assigns a path γ_0 in Gr_g by considering pullback of $T(T_{\boldsymbol{\alpha}}) \subset T\,\mathrm{Sym}^g(\Sigma)$ applying the trivialization of $\varphi^*(T\,\mathrm{Sym}^g(\Sigma))$ once again. Analogously, we get a path γ_1. Finally, the Maslov index $\mu(\varphi)$ is equal to a composition of all these four paths

$$\mu(\varphi) = [\gamma_{\boldsymbol{x}} \circ \gamma_0 \circ \gamma_{\boldsymbol{y}} \circ \gamma_1] \in H_1(\mathrm{Gr}_g) = \mathbb{Z}.$$

We also introduce the *combinatorial index* of any domain $D \in \mathfrak{D}(\boldsymbol{x}, \boldsymbol{y})$. For $x_i \in \boldsymbol{x}$ define $\widetilde{\mu}_{x_i}(D)$ as the average of the coefficients of D in the 4 regions to which x_i belongs. Then the *point measure* of D at $\boldsymbol{x}$ is $\widetilde{\mu}_x(D) = \sum_{i=1}^{g} \widetilde{\mu}_{x_i}(D)$. For a 2–chain D the Euler measure D is $\frac{1}{2\pi}$ of the integral of the curvature of the metric of Σ over D. It is equal to the 2–cochain that assigns $\frac{1}{2}(2-n)$ to a $2n$–gon region. For a domain $D \in \mathfrak{D}(\boldsymbol{x}, \boldsymbol{y})$ we assign its combinatorial index by

$$\widetilde{\mu}(D) = \widetilde{\mu}_{\boldsymbol{x}}(D) + \widetilde{\mu}_{\boldsymbol{y}}(D) + e(D).$$

2.2 Transformations of Heegaard diagrams

We introduce two types of transformations on a given Heegaard diagram $(\Sigma, \boldsymbol{\alpha}, \boldsymbol{\beta})$ that are used in this paper.

Definition 2.2 Let γ be an oriented path in Σ which is transverse to $\boldsymbol{\alpha}$ and $\boldsymbol{\beta}$ and is disjoint from $\boldsymbol{\alpha} \cap \boldsymbol{\beta}$; see Figure 1. Also, assume the endpoints p_0 and p_1 of γ do not belong to $\boldsymbol{\alpha} \cup \boldsymbol{\beta}$. Let U be a small neighborhood of γ. Let ψ be an isotopy of Σ supported on U which moves $\boldsymbol{\alpha}$ curves in the direction of γ as given in Figure 1. The *finger move* on the $\boldsymbol{\alpha}$ curves along the curve γ is a restriction $\psi|_{\alpha}$; this does not move the $\boldsymbol{\beta}$ curves. Analogously we define the *finger move on the $\boldsymbol{\beta}$ curves*.

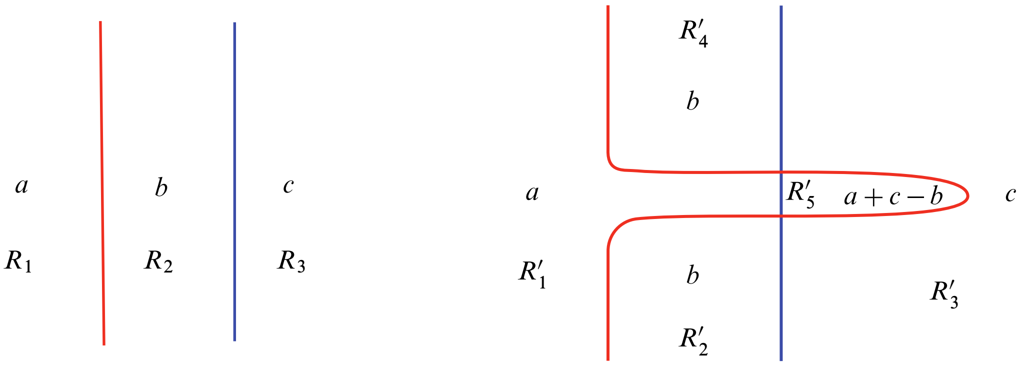

Figure 2: Image of a domain.

A transition from a Heegaard diagram $(\Sigma, \boldsymbol{\alpha}, \boldsymbol{\beta})$ to the diagram $(\Sigma, \psi(\boldsymbol{\alpha}), \boldsymbol{\beta})$ will be called by *performing a finger move on* $\boldsymbol{\alpha}$ *along* γ. Finger moves were introduced in [Sarkar and Wang 2010].

Definition 2.3 Given a domain D, its *image* $D' = \psi(D)$ under a finger move ψ is defined as follows. First decompose a finger move ψ into a sequence $\psi = \psi_1 \circ \cdots \circ \psi_m$ of finger moves where under any ψ_i only two new points of intersection between $\boldsymbol{\alpha}$ and $\boldsymbol{\beta}$ appear (see Figure 2). Let R_1, R_2 and R_3 be regions at which $\psi_1 \circ \cdots \circ \psi_{i-1}(D)$ has coefficients a, b and c, respectively, and let the finger move ψ_i be as shown in the picture. Then for new regions R_1', R_2', R_3', R_4' and R_5' shown in Figure 2 the coefficients are a, b, c, b and $a+c-b$ as shown. Repeating this procedure gives us $\psi(D)$.

Definition 2.4 Let D be a domain of a Heegaard diagram $(\Sigma, \boldsymbol{\alpha}, \boldsymbol{\beta})$. We call an *empty stabilization* of this Heegaard diagram with respect to D a stabilization which is obtained by taking the connected sum with the standard genus 1 Heegaard diagram for S^3 where the attaching disk belongs to a region of $(\Sigma, \boldsymbol{\alpha}, \boldsymbol{\beta})$ and the coefficient of D is equal to 0. The new Heegaard diagram $(\Sigma', \boldsymbol{\alpha}', \boldsymbol{\beta}')$ is also called an *empty stabilization* of $(\Sigma, \boldsymbol{\alpha}, \boldsymbol{\beta})$. The image of D under an empty stabilization is D itself in the new diagram.

If we are given a Whitney disk $\varphi \in \pi_2(\boldsymbol{x}, \boldsymbol{y})$ we may define its *image* φ' under a finger move on $\boldsymbol{\alpha}$ by isotoping φ in accordance with the induced isotopy of $T_{\boldsymbol{\alpha}}$ inside $\mathrm{Sym}^g(\Sigma)$. Analogously, one defines the image of φ under a finger move on $\boldsymbol{\beta}$.

We say that the stabilization is empty with respect to a Whitney disk φ if it is empty with respect to $D(\varphi)$. For the empty stabilization with respect to φ the image of φ is just $\varphi \times z$ where z is the intersection point of added α_{g+1} and β_{g+1}.

We will extensively use the invariance of the Maslov index and of $\tilde{\mu}$ under these two types of transformations of a Heegaard diagram which is shown in the lemma below.

Lemma 2.5 *Let $D \in \mathfrak{D}(\boldsymbol{x}, \boldsymbol{y})$ be a domain in a Heegaard diagram $(\Sigma, \boldsymbol{\alpha}, \boldsymbol{\beta})$ and let $\varphi \in \pi_2(\boldsymbol{x}, \boldsymbol{y})$ be a Whitney disk. Let D' be the image of D under a finger move or an empty stabilization with respect* *to D. Let φ' be the image of φ under a finger move or an empty stabilization with respect to φ. Then $\mu(\varphi) = \mu(\varphi')$ and $\widetilde{\mu}(D) = \widetilde{\mu}(D')$.*

Proof First, consider the case when this transformation is an empty stabilization with respect to D (or φ). Let α_{g+1} and β_{g+1} be two new curves of $(\Sigma, \boldsymbol{\alpha}', \boldsymbol{\beta}')$ and z be their point of intersection. We have $\boldsymbol{x}' = \boldsymbol{x} \cup \{z\}$, $\boldsymbol{y}' = \boldsymbol{y} \cup \{z\}$ and $D' = D \in \mathfrak{D}(\boldsymbol{x}', \boldsymbol{y}')$ (or $\varphi' \in \pi_2(\boldsymbol{x}', \boldsymbol{y}')$). First, $\widetilde{\mu}(D) = \widetilde{\mu}(D')$, because $\widetilde{\mu}_z(D') = 0$. As for the Maslov index, notice that paths γ_0 and γ_1 in Gr_g rise to paths γ_0' and γ_1' in Gr_{g+1} obtained by taking direct sum with one-dimensional real subspaces of $\mathbb{R}^{2(g+1)} = \mathbb{C}^{g+1}$ corresponding to $T_z\alpha_{g+1}$ and $T_z\beta_{g+1}$ respectively. Hence $\mu(\varphi) = \mu(\varphi')$.

If the transformation is a finger move then the Maslov indices are equal because finger move keeps $\boldsymbol{\alpha}$ and $\boldsymbol{\beta}$ unchanged near $\boldsymbol{x}$ and $\boldsymbol{y}$. Hence, inspecting the definition of Maslov indices we see that only the paths in Gr_g coming from the boundary ∂D^2 differ, and they are isotopic to the initial ones, so the class in $H_1(\mathrm{Gr}_g)$ does not change. Finally, $\widetilde{\mu}(D) = \widetilde{\mu}(D')$ is immediate from the formula (see also [Sarkar 2011, Theorem 3.4]). □

2.3 Additivity of indices

Our strategy for proving Lipshitz's formula is based on decomposing any domain into the composition of trivial pieces: bigons and rectangles. To apply this decomposition we need the additivity of the Maslov index μ and of the combinatorial index $\widetilde{\mu}$ under the composition of domains. It is generally known that the Maslov index μ is additive. It was shown in more generality in [Sarkar 2011, Theorem 3.3] that $\widetilde{\mu}$ is additive and here we repeat the proof in our terms.

Definition 2.6 Let γ_1 and γ_2 be oriented 1–chains in Σ supported on $\boldsymbol{\alpha} \cup \boldsymbol{\beta}$ and intersecting transversely. Denote by $\gamma_1 \cdot \gamma_2$ the intersection number of these 1–chains, which is equal to the signed count of intersection points where the sign is defined by comparing the orientation of Σ and the orientation coming from γ_1 and γ_2. A contribution to the intersection number at an endpoint is given by a fraction $\pm\frac{1}{2}$ or $\pm\frac{1}{4}$ as in [Sarkar 2011, Section 2].

Lemma 2.7 *Let $D \in \mathfrak{D}(\boldsymbol{x}, \boldsymbol{y})$ and D' be any other 2–chain in the Heegaard diagram $(\Sigma, \boldsymbol{\alpha}, \boldsymbol{\beta})$. Then $\widetilde{\mu}_{\boldsymbol{y}}(D') - \widetilde{\mu}_{\boldsymbol{x}}(D') = \partial D|_{\boldsymbol{\alpha}} \cdot \partial D'|_{\boldsymbol{\beta}} = \partial D'|_{\boldsymbol{\alpha}} \cdot \partial D|_{\boldsymbol{\beta}}$.*

Proof Given orientations on $\boldsymbol{\alpha}$ at each intersection point p between $\boldsymbol{\alpha}$ and $\boldsymbol{\beta}$ we give numbers to regions from *I* to *IV*. Namely, quadrants *I* and *II* are in the upper half of $\boldsymbol{\beta}$ (the half in the positive direction of $\boldsymbol{\alpha}$) and quadrant *I* is the one for which the orientation induced from Σ is opposite to the orientation of $\boldsymbol{\alpha}$ at p. Quadrants *III* and *IV* are defined following *II* in the counterclockwise order on Σ.

Let us pick a point p in the first quadrant near the point $x_i \in \boldsymbol{x}$ lying on some α_k and travel parallel to $\partial D|_{\boldsymbol{\alpha}_k}$ until we reach a first quadrant near $y_j \in \boldsymbol{y}$ where $\partial(\partial D|_{\boldsymbol{\alpha}_k}) = y_j - x_i$. Then let us track the coefficient of D' at each point along this path. Each time we change the region passing through $\boldsymbol{\beta}$ this coefficient changes by the intersection number of this small portion of our path with $\partial D'|_{\boldsymbol{\beta}}$. Hence, the difference between the coefficients is equal to $\partial D|_{\alpha_k} \cdot \partial D'|_{\boldsymbol{\beta}}$.

Now, by taking such paths for all points in $\boldsymbol{x}$ and all 4 quadrants for each of these points and then averaging we get $\widetilde{\mu}_{\boldsymbol{y}}(D') - \widetilde{\mu}_{\boldsymbol{x}}(D') = \partial D|_{\boldsymbol{\alpha}} \cdot \partial D'|_{\boldsymbol{\beta}}$. □

Corollary 2.8 *Let $D \in \mathfrak{D}(\boldsymbol{x}, \boldsymbol{y})$ and $D' \in \mathfrak{D}(\boldsymbol{y}, \boldsymbol{z})$. Then $\widetilde{\mu}(D * D') = \widetilde{\mu}(D) + \widetilde{\mu}(D')$.*

Proof First, we easily see that

$$\widetilde{\mu}(D * D') - \widetilde{\mu}(D) - \widetilde{\mu}(D') = \widetilde{\mu}_{\boldsymbol{x}}(D') + \widetilde{\mu}_{\boldsymbol{z}}(D) - \widetilde{\mu}_{\boldsymbol{y}}(D') - \widetilde{\mu}_{\boldsymbol{y}}(D).$$

Second, applying Lemma 2.7 we get $\widetilde{\mu}_{\boldsymbol{y}}(D') - \widetilde{\mu}_{\boldsymbol{x}}(D') = \partial D|_{\boldsymbol{\alpha}} \cdot \partial D'|_{\boldsymbol{\beta}}$ and $\widetilde{\mu}_{\boldsymbol{z}}(D) - \widetilde{\mu}_{\boldsymbol{y}}(D) = \partial D|_{\boldsymbol{\alpha}} \cdot \partial D'|_{\boldsymbol{\beta}}$.

Hence,

$$\widetilde{\mu}(D * D') - \widetilde{\mu}(D) - \widetilde{\mu}(D') = 0.$$ □

3 Main theorem

Theorem 3.1 *For a given domain D in a Heegaard diagram $(\Sigma, \boldsymbol{\alpha}, \boldsymbol{\beta})$ there is a sequence of finger moves and empty stabilizations such that in the new Heegaard diagram the image of D can be represented as a composition of bigons, rectangles and their negatives.*

Before proving this theorem we show how Theorems 1.1 and 1.2 follow from Theorem 3.1.

Proof of Theorem 1.1 Let $D \in \mathfrak{D}(\boldsymbol{x}, \boldsymbol{y})$. Apply Theorem 3.1 to obtain the image D' of D and the decomposition $D' = D_1 * \cdots * D_k$ of D' in the new Heegaard diagram. Here each D_i is either a bigon, a rectangle, or the negative of a bigon or a rectangle. Since $\overline{\mu}$ is additive we may compute $\overline{\mu}(D') = \overline{\mu}(D_1) + \cdots + \overline{\mu}(D_k)$. For each D_i the value $\overline{\mu}(D_i)$ can be easily inferred from the 4 axioms.

The fact that $\overline{\mu}$ coincides with $\widetilde{\mu}$ then follows since $\widetilde{\mu}(R) = \widetilde{\mu}(B) = 1$ by direct computation, and $\widetilde{\mu}$ is additive by Lemma 2.7 and stable by Lemma 2.5. □

Proof of Theorem 1.2 We are given a Whitney disk $\varphi \in \pi_2(\boldsymbol{x}, \boldsymbol{y})$ and we may assume that $g(\Sigma) > 1$ by applying an empty stabilization if necessary. By Theorem 3.1 there is a transformation of the given Heegaard diagram such that there is a decomposition $D(\varphi') = D_1 * \cdots * D_k$, where φ' is an image of φ under this transformation; equivalently $0 = D(\varphi') * (-D_1) * \cdots * (-D_k)$. Since each D_i is either a bigon or a rectangle (possibly negative) there exists a corresponding Whitney disk φ_i such that $D(\varphi_i) = -D_i$. Then $\varphi' * \varphi_1 * \cdots * \varphi_k \in \pi_2(\boldsymbol{x}, \boldsymbol{x})$ and, moreover, $D(\varphi' * \varphi_1 * \cdots * \varphi_k) = 0$. From [Ozsváth and Szabó 2004b, Proposition 2.15] it now follows that $\varphi' * \varphi_1 * \cdots * \varphi_k = 0 \in \pi_2(\boldsymbol{x}, \boldsymbol{x})$, so $\mu(\varphi' * \varphi_1 * \cdots * \varphi_k) = 0$. Hence, $\mu(\varphi') = -(\mu(\varphi_1) + \cdots + \mu(\varphi_k))$.

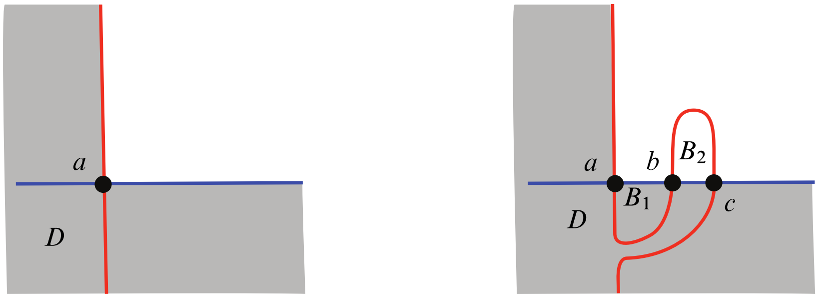

Figure 3: 270° angle.

It now suffices to show that $\mu(B) = \tilde{\mu}(B) = 1$ and $\mu(R) = \tilde{\mu}(R) = 1$ for any bigon B and any rectangle R. For a bigon $\mu(B) = 1$ since it agrees with the dimension of the (regular) moduli space of biholomorphisms from B to the strip $[0,1] \times \mathbb{R}$. The fact that $\mu(R) = 1$ is shown in [Ozsváth and Szabó 2004b, Section 8.4]. □

Now we prove the main theorem.

Proof of Theorem 3.1 In the proof we abuse notation and denote the image of a domain D under any empty stabilization or a finger move by same letter D.

We break our proof into several steps starting with a general domain in Step 1 and simplifying it gradually by transformations of Heegaard diagrams. Before we start dealing with general domains we need additional preparation which we perform at Step 0.

Step 0: quadrilaterals Before considering the most general domains we need to take care of another type of a "building block". Namely, let D be an embedded domain with nonnegative coefficients which is homeomorphic to a disk and has a boundary consisting of four sides. We would call such D a *quadrilateral*. If all angles of D are 90° then it is already a rectangle. Otherwise, an angle at one of its vertices a is 270°. Consider a finger move shown in Figure 3 which creates two bigons $B_1 \in \pi_2(a,b)$ and $B_2 \in \pi_2(b,c)$. Then $D * (-B_1)$ is a quadrilateral with one more 90° angle than D. Proceeding in the same fashion we decompose D into a rectangle and several bigons with possibly some $\boldsymbol{x}$– or $\boldsymbol{y}$–coordinates in the interiors. We refer the reader to Step 5 for the treatment of these inner points.

Henceforth, in the following steps it is enough to decompose any domain into quadrilaterals and bigons with arbitrary angles.

Step 1: making the boundary embedded First, we show that after several finger moves we may compose D with some bigons (or their negatives) and obtain a domain D' with embedded boundary.

Assume without loss of generality that $\partial(\partial D|_{\alpha_1}) = y_1 - x_1$ with respect to the chosen orientation on α_1. Here x_1 lies on β_1 and y_1 lies on β_2 (where β_2 may be equal to β_1). We may assume that the positively oriented embedded arc from x_1 to y_1 in α_1 is covered $k+1$ times by ∂D and the positively oriented embedded arc from y_1 to x_1 is covered k times. For now assume $k > 0$.

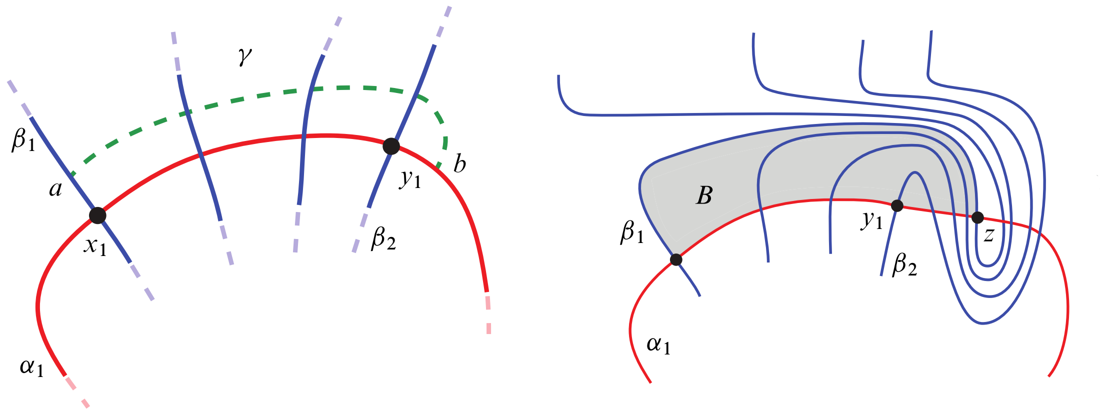

Figure 4: Making the boundary embedded.

Since the $\boldsymbol{\alpha}$ and $\boldsymbol{\beta}$ curves are oriented, for any region we may distinguish whether it lies to the left of a given $\boldsymbol{\alpha}$ or $\boldsymbol{\beta}$ curve. Let a be a point very close to x_1 on β_1 to the left of α_1 (see Figure 4). Also let b be a point on α_1 near y_1 not belonging to the positive arc from x_1 to y_1. Let γ be (a slight extension of) a curve starting at a and parallel to α_1 until it hits β_2 and then we connect it with b. We make a finger move on $\boldsymbol{\beta}$ curves along the curve γ creating new points of intersection of $\boldsymbol{\beta}$ curves intersecting γ (including β_1 and β_2) with α_1. Let z be the new intersection point of β_1 and α_1 which is the closest to x_1 on β_1.

As a result, we created a bigon B connecting x_1 to z. Then

$$D' = (-B) * D \in \mathfrak{D}(\{z, x_2, \dots, x_g\}, \{y_1, y_2, \dots, y_g\}).$$

Note that in $\partial D'$ the arc from z to y_1 is covered k times and the arc from y_1 to z is covered $k-1$ times. Additionally, we notice that $\partial D'|_{\boldsymbol{\beta}}$ only changed by replacing x_1 with z which may be assumed to be very close to x_1 on β_1 and hence the number of times $\partial D'_{\boldsymbol{\beta}}$ covers z doesn't differ from that of x_1 for the former D. Hence performing isotopies as above only changes the geometry of the α_1–portion of ∂D.

In the case $k < 0$ we would draw γ parallel to the negative embedded arc from x_1 to y_1 and proceed analogously. Repeating this procedure we first make sure that $\partial D \cap \boldsymbol{\alpha}$ is embedded and then we repeat it for $\boldsymbol{\beta}$ and end up with a domain having an embedded boundary.

Step 2: making the boundary connected Assume the boundary of a domain D consists of more than one closed curve as shown in Figure 5. Suppose $\partial D \cap (\alpha_1 \cap \beta_1) = y_1$, $\partial D \cap (\beta_1 \cap \alpha_2) = x_2$ and $\partial(\partial D|_{\alpha_2}) = y_2 - x_2$. Let us pick a point on α_1 close to y_1 and let γ be an arc connecting it to a point on the restriction of some other component of ∂D to $\boldsymbol{\beta}$ such that $\operatorname{int}(\gamma)$ does not intersect ∂D. We denote by β_1' the curve to which the endpoint of γ belongs and $\partial(\partial D|_{\beta_1'}) = x_2' - y_1'$ while $\partial(\partial D|_{\alpha_1'}) = y_1' - x_1'$. We also can make sure that γ intersects β_1' at a point near y_1'.

Let us decompose $\gamma = \gamma_1\gamma_2\gamma_3$ where γ_1 and γ_3 are small portions near the ends and γ_2 is the remaining portion in the middle. We draw a curve γ_1' connecting a point near y_1 on β_1 with some point near the end of γ_1 such that γ_1' does not intersect γ_1. Starting at the end of γ_1', we draw a curve γ_2' parallel to γ_2. Then

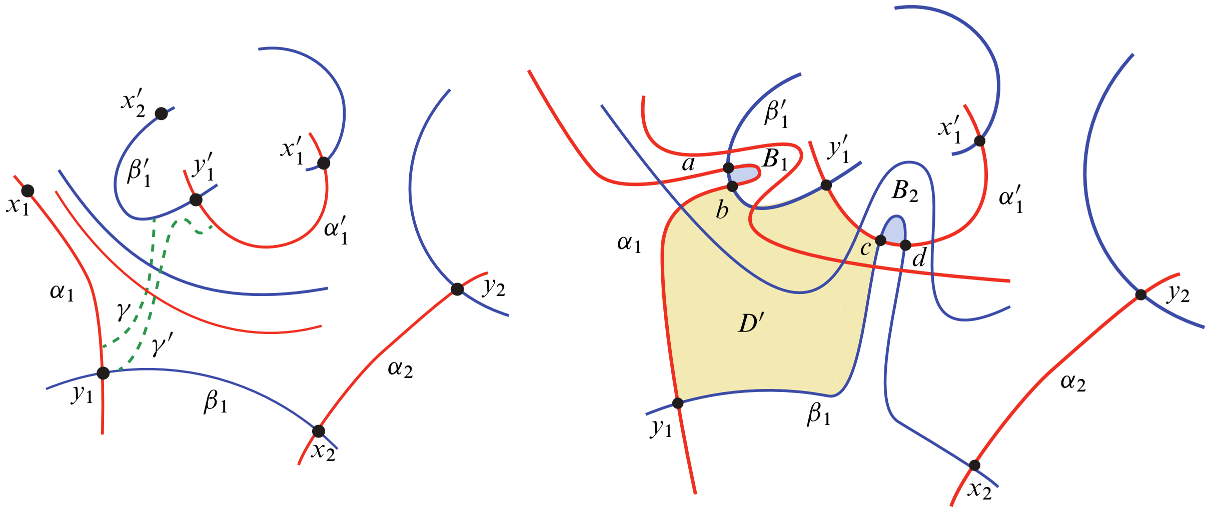

Figure 5: Making the boundary connected.

we connect the end of γ_2' by a curve γ_3' parallel to β_1' with a point on α_1' near y_1'. We set $\gamma' = \gamma_1'\gamma_2'\gamma_3'$. In short, γ' is a parallel copy of γ on the complement of neighborhoods of points y_1 and y_1'.

Now we make a finger move on $\boldsymbol{\alpha}$ curves along γ and we also make a finger move on $\boldsymbol{\beta}$ curves along γ'. Denote the new points of intersection between α_1 and β_1' by a and b, and analogously denote the points of intersection between β_1 and α_1' by c and d.

Denote the new quadrilateral by $D' \in \mathfrak{D}(\{b, c\}, \{y_1, y_1'\})$ and the two new bigons by $B_1 \in \mathfrak{D}(\{a\}, \{b\})$ and $B_2 \in \mathfrak{D}(\{c\}, \{d\})$.

Then consider

$$D * (-D') * B_1 * B_2 \in \mathfrak{D}(\boldsymbol{x}, \{a, y_2', \dots, d, y_2, \dots\})$$

whose boundary is embedded and contains one fewer component than D. From here we may proceed inductively on the number of boundary components.

Step 3: reducing to a quadrangle or a bigon boundary Let D be a domain. Applying Steps 1 and 2, we assume that ∂D is embedded and connected.

Let the boundary of a domain D be $2n$–sided, ie of the form $x_1 y_1 x_2 y_2 x_3 \cdots y_n$ with $n > 2$ where $x_i y_i$ is an arc on $\boldsymbol{\alpha}$ and $y_i x_{i+1}$ is an arc on $\boldsymbol{\beta}$. Assume that the first 4 sides lie on α_1, β_1, α_2 and β_2 (see Figure 6). Let us pick a point y_1' on $x_1 y_1$ near y_1 and a point y_2' on β_2 near y_2. Let γ be an arc connecting y_1' and y_2' such that $\mathrm{int}(\gamma) \cap \partial D = \varnothing$ and the arcs γ, $y_1 y_1'$, $y_1 x_2$, $x_2 y_2$ and $y_2 y_2'$ bound an embedded disk. We make a finger move on $\boldsymbol{\alpha}$ curves along γ and denote by a and b two new points of intersection between α_1 and β_2. Notice that we created two new domains: a bigon $B \in \mathfrak{D}(\{a\}, \{b\})$ and a quadrilateral $D' \in \mathfrak{D}(\{x_2, b\}, \{y_1, y_2\})$.

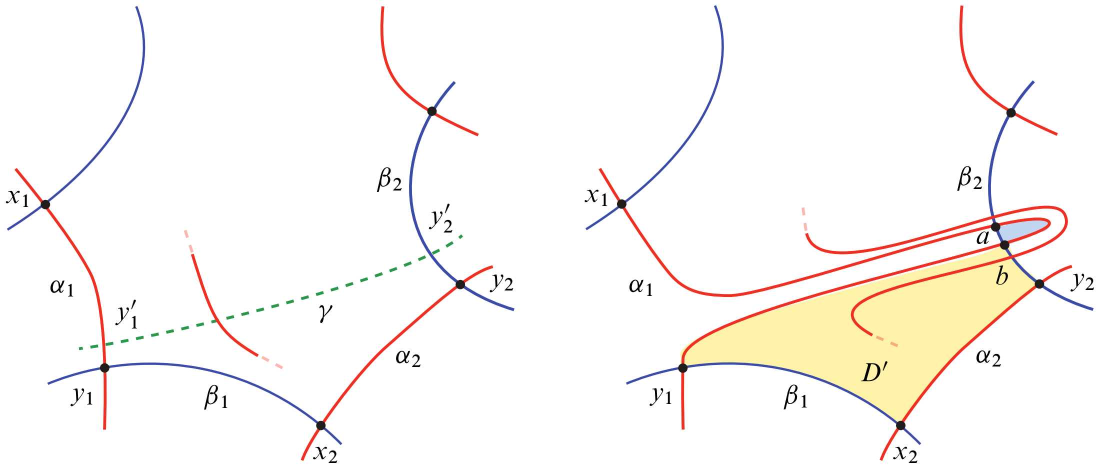

Figure 6: Decreasing the number of sides.

We may replace D with a domain

$$D * (-D') * B \in \pi_2(\{x_1, x_2, \dots, x_n\}, \{a, x_2, y_3, \dots, y_n\}),$$

which has an embedded and connected boundary with $2n-2$ sides.

Step 4a: 4–sided boundary Given two domains which have the same 4–sided curve as the boundary, their difference is an element in $H_2(\Sigma)$ which is generated by $[\Sigma]$. We will prove in Claim 3.2 that Σ can be decomposed into bigons and rectangles after some finger moves and empty stabilizations. Therefore we may add $k[\Sigma]$ to a given domain D to ensure that we get a domain represented by an embedded 2–chain. This domain, which we also call D, is isotopic to a disk with m handles.

We will now show how to decompose this handlebody D into bigons and quadrilaterals.

We depict handles as pairs of circles with opposite orientations and one of the handles is drawn in Figure 7. We now draw two "palm trees" as in the picture by making two finger moves on $\boldsymbol{\alpha}$ curves and we assume that the other $m-1$ handles are in the white region "between" two palm trees. Let the 8 new points of intersection between the $\boldsymbol{\alpha}$ and $\boldsymbol{\beta}$ curves be labeled as in Figure 7.

We now have 4 new bigons B_{11}, B_{12}, B_{21} and B_{22}, and 2 new quadrilaterals R_x and R_y. Then the domain $D * (-R_x) * (-R_y) * B_{11} * B_{12} * B_{21} * B_{22} \in \mathfrak{D}(\{z_1', z_2'\}, \{w_1', w_2'\})$ has 4–sided boundary and $m-1$ handles and from here proceed inductively on the number of handles.

Step 4b: 2–sided boundary Here we reduce this case to the 4–sided boundary case treated in Step 4a.

As in the 4–sided boundary case, we may assume D to be an embedded 2–chain represented by a handlebody as shown in Figure 8. By the method of Step 0 we may assume that both angles are $90°$.

We may assume that $g \geqslant 2$ by applying an empty stabilization with respect to D if necessary. Let $D \in \mathfrak{D}(\{x, z_1, \dots, z_{g-1}\}, \{y, z_1, \dots, z_{g-1}\})$. We may suppose $z_1 \in \alpha_2 \cap \beta_2$ lies outside of D by applying

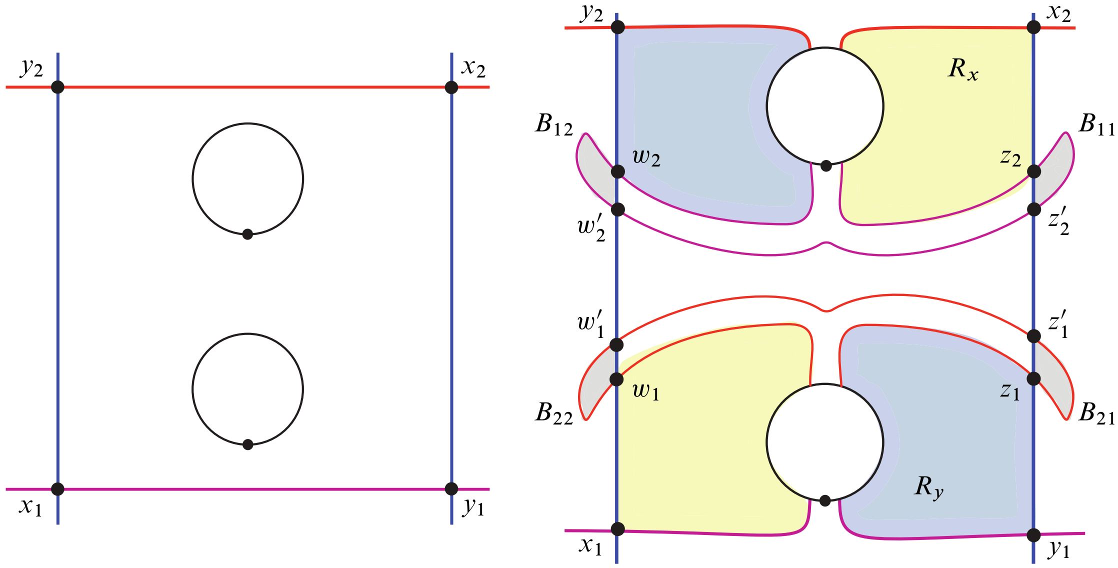

Figure 7: 4–sided boundary.

an empty stabilization with respect to a given D. Let γ be an arc connecting the point z_1 with some point a on the boundary of D such that γ intersects D once at the point a. We may assume a to be somewhere on β_1. We also alter the path γ slightly so that it starts at some point on α_2 and β_2 is to its left near this endpoint.

Now draw γ' almost parallel to γ so that one of its endpoints is on β_2 near z_1. When γ' reaches a neighborhood of a we extend it parallel to $-\beta_2$ until it hits α_1 at some point outside of D near y.

We make a finger move on $\boldsymbol{\alpha}$ along γ and a finger move on $\boldsymbol{\beta}$ along γ' creating points $b \in \alpha_2 \cap \beta_1$ and $c \in \beta_2 \cap \alpha_1$. There is now a new quadrilateral $R \in \mathcal{D}(\{y, z_1, z_2, \dots, z_{g-1}\}, \{b, c, \dots, z_{g-1}\})$.

Therefore, we may replace D with $D * R \in \mathcal{D}(\{x, z_1, z_2, \dots, z_{g-1}\}, \{b, c, \dots, z_{g-1}\})$ reducing to Step 4a since it has connected and embedded 4–sided boundary.

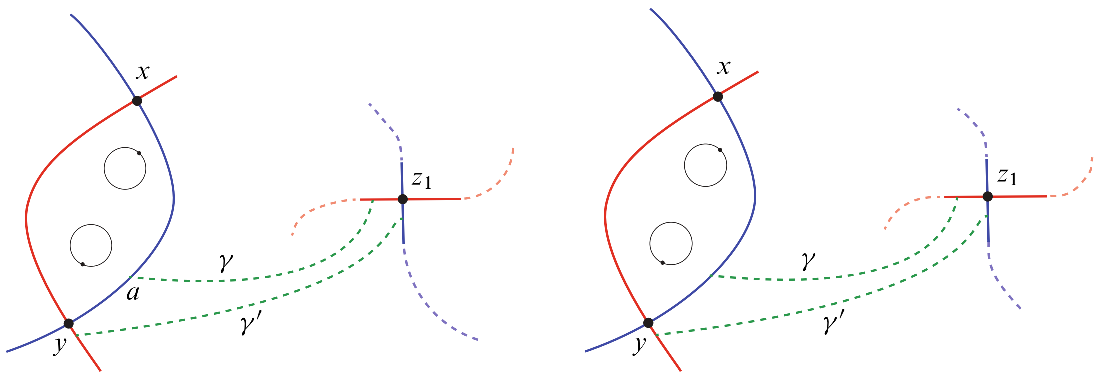

Figure 8: 2–sided boundary.

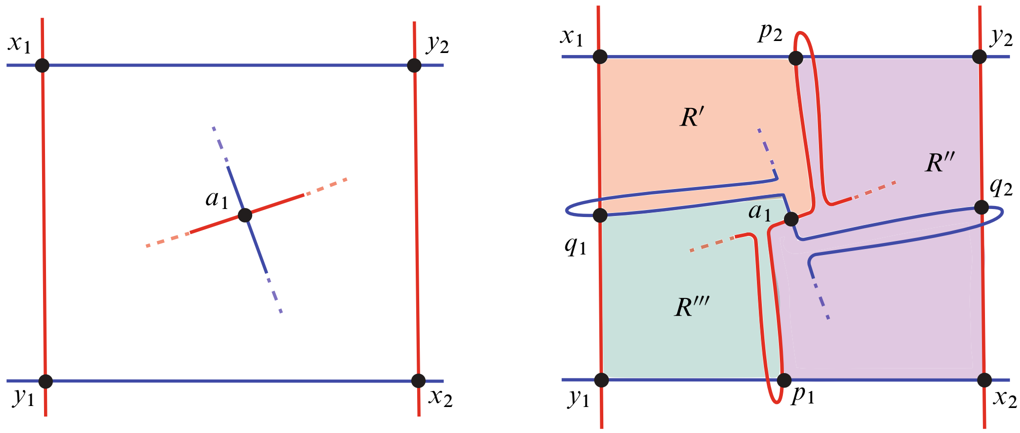

Figure 9: Inner points.

Step 5: inner points By now we have represented the initial D as a composition of domains that geometrically look like bigons and rectangles, but some of the rectangles may contain some points from generators inside of them. Namely, let $R \in \mathfrak{D}(\boldsymbol{x}, \boldsymbol{y})$ where $\boldsymbol{x} = \{x_1, x_2, a_1, \dots, a_k, b_{k+1}, \dots, b_{g-2}\}$ and $\boldsymbol{y} = \{y_1, y_2, a_1, \dots, a_k, b_{k+1}, \dots, b_{g-2}\}$ where the a_i lie inside of R and the b_j lie outside of R.

Let $a_1 \in \alpha_3 \cap \beta_3$. We make finger moves on α_3 and β_3, creating 2 points of intersection between α_3 and β_1, β_2, and 2 points of intersection between β_3 and α_1, α_2 (actually, we created twice as many points, but we stress our attention on these 4). We call these points p_1, p_2, q_1 and q_2, respectively. This is illustrated in Figure 9.

Then we may see that $R = R' * R'' * R'''$ where

$$R' \in \mathfrak{D}(\boldsymbol{x}, \{q_1, x_2, p_2, a_2, \dots, a_k, b_{k+1}, \dots, b_g\}),$$
$$R'' \in \mathfrak{D}(\{q_1, x_2, p_2, a_2, \dots, a_k, b_{k+1}, \dots, b_g\}, \{q_1, y_2, p_1, \dots, a_k, b_{k+1}, \dots, b_g\}),$$
$$R''' \in \mathfrak{D}(\{q_1, x_2, p_1, a_2, \dots, a_k, b_{k+1}, \dots, b_g\}, \boldsymbol{y}).$$

Each of these 3 rectangles has fewer points from generators inside than R and we may proceed by induction on the number of points.

This completes the proof of Theorem 3.1, assuming Claim 3.2 below. □

Claim 3.2 *The surface $\Sigma \in \mathfrak{D}(\boldsymbol{x}, \boldsymbol{x})$ for $\boldsymbol{x} = \{x_1, \dots, x_g\}$ is a domain that can be decomposed into bigons and rectangles after applying a sequence of finger moves.*

Proof Let us assume $g > 1$. We may apply a diffeomorphism φ to the Heegaard diagram $(\Sigma, \boldsymbol{\alpha}, \boldsymbol{\beta})$ such that the image of $\boldsymbol{x}$ is a collection $\boldsymbol{x}'$ such that all x_i' are located in some small disk region and x_1' and x_2' are on the boundary of the convex hull of $\boldsymbol{x}'$. Let us denote by $(\Sigma, \boldsymbol{\alpha}', \boldsymbol{\beta}')$ the image of the initial diagram under φ, ie $\boldsymbol{\alpha}' = \varphi(\boldsymbol{\alpha})$ and $\boldsymbol{\beta}' = \varphi(\boldsymbol{\beta})$. We may assume that $x_1' \in \alpha_1' \cap \beta_2'$ and $x_2' \in \alpha_2' \cap \beta_1'$. Then we make finger moves on α_1', α_2' and on β_1', β_2' as in Figure 10, creating a rectangle R with boundary

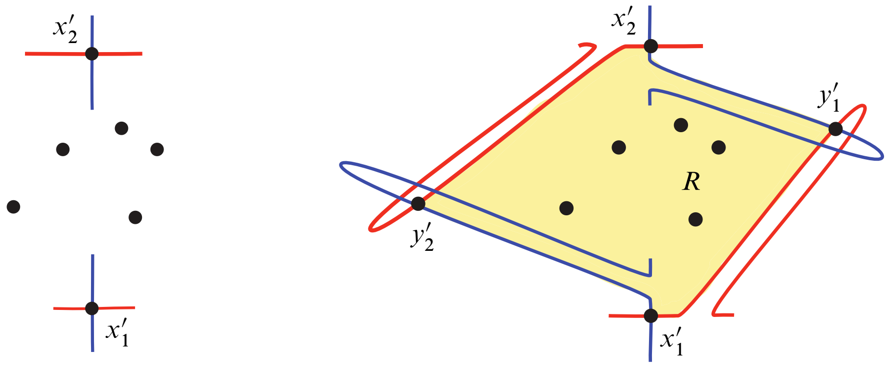

Figure 10: Claim 3.2.

$x_1' y_1' x_2' y_2'$ such that all other points of $\boldsymbol{x}'$ are inside of R. Then $\Sigma * (-R)$ connects $\boldsymbol{x}'$ to $\{y_1', y_2', \dots, x_g'\}$ and it is a region with quadrangle boundary and g handles. Now we may proceed as in Step 4a of the proof of the theorem.

Let $g = 1$. We can make a finger move on α_1 which creates a bigon B connecting given point x to some point x'. Then $(-B) * \Sigma \in \mathfrak{D}(\{x'\}, \{x\})$. Now we make a stabilization inside B and can proceed as in the proof of Step 4b. □

References

[Ghiggini 2008] **P Ghiggini**, *Knot Floer homology detects genus-one fibred knots*, Amer. J. Math. 130 (2008) 1151–1169 MR Zbl

[Lipshitz 2006] **R Lipshitz**, *A cylindrical reformulation of Heegaard Floer homology*, Geom. Topol. 10 (2006) 955–1096 MR Zbl Correction in 18 (2014) 17–30

[Ni 2009a] **Y Ni**, *Heegaard Floer homology and fibred 3–manifolds*, Amer. J. Math. 131 (2009) 1047–1063 MR Zbl

[Ni 2009b] **Y Ni**, *Link Floer homology detects the Thurston norm*, Geom. Topol. 13 (2009) 2991–3019 MR Zbl

[Ozsváth and Szabó 2004a] **P Ozsváth**, **Z Szabó**, *Holomorphic disks and genus bounds*, Geom. Topol. 8 (2004) 311–334 MR Zbl

[Ozsváth and Szabó 2004b] **P Ozsváth**, **Z Szabó**, *Holomorphic disks and topological invariants for closed three-manifolds*, Ann. of Math. 159 (2004) 1027–1158 MR Zbl

[Ozsváth and Szabó 2004c] **P Ozsváth**, **Z Szabó**, *Holomorphic disks and three-manifold invariants: properties and applications*, Ann. of Math. 159 (2004) 1159–1245 MR Zbl

[Ozsváth and Szabó 2006] **P Ozsváth**, **Z Szabó**, *Holomorphic triangles and invariants for smooth four-manifolds*, Adv. Math. 202 (2006) 326–400 MR Zbl

[Rasmussen 2003] **J A Rasmussen**, *Floer homology and knot complements*, PhD thesis, Harvard University (2003) arXiv math/0306378

[Sarkar 2011] **S Sarkar**, *Maslov index formulas for Whitney n–gons*, J. Symplectic Geom. 9 (2011) 251–270 MR Zbl

[Sarkar and Wang 2010] **S Sarkar**, **J Wang**, *An algorithm for computing some Heegaard Floer homologies*, Ann. of Math. 171 (2010) 1213–1236 MR Zbl

[Seidel 2008] **P Seidel**, *Fukaya categories and Picard–Lefschetz theory*, Eur. Math. Soc., Zürich (2008) MR Zbl

Department of Mathematics, University of California, Los Angeles
Los Angeles, CA, United States

romankrut@ucla.edu

Received: 4 July 2022 Revised: 30 April 2023

ALGEBRAIC & GEOMETRIC TOPOLOGY

msp.org/agt

See inside back cover or msp.org/agt for submission instructions.

The subscription price for 2024 is US $705/year for the electronic version, and $1040/year (+$70, if shipping outside the US) for print and electronic. Subscriptions, requests for back issues and changes of subscriber address should be sent to MSP. Algebraic & Geometric Topology is indexed by Mathematical Reviews, Zentralblatt MATH, Current Mathematical Publications and the Science Citation Index.

Algebraic & Geometric Topology (ISSN 1472-2747 printed, 1472-2739 electronic) is published 9 times per year and continuously online, by Mathematical Sciences Publishers, c/o Department of Mathematics, University of California, 798 Evans Hall #3840, Berkeley, CA 94720-3840. Periodical rate postage paid at Oakland, CA 94615-9651, and additional mailing offices. POSTMASTER: send address changes to Mathematical Sciences Publishers, c/o Department of Mathematics, University of California, 798 Evans Hall #3840, Berkeley, CA 94720-3840.

AGT peer review and production are managed by EditFlow® from MSP.

PUBLISHED BY

mathematical sciences publishers

nonprofit scientific publishing

https://msp.org/

ALGEBRAIC & GEOMETRIC TOPOLOGY

Volume 24 Issue 8 (pages 4139–4730) 2024
